nature portfolio

https://doi.org/10.1038/s41586-025-09548-0

Supplementary information

Co-option of an ancestral cloacal regulatory landscape during digit evolution

In the format provided by the authors and unedited

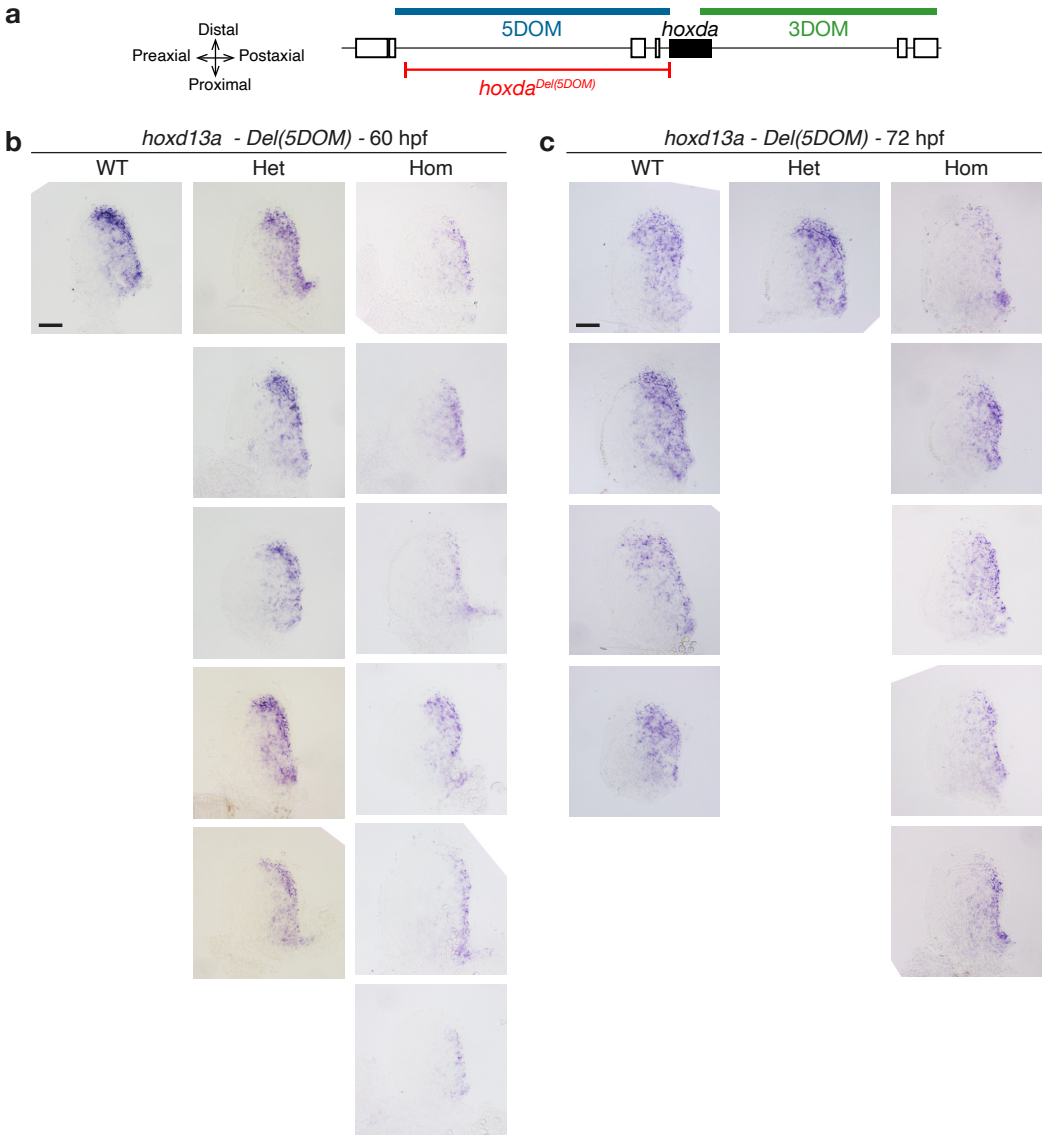

Supplementary Figure 1. *hoxd13a* expression in control, heterozygous and homozygous mutant fin buds at 60 and 72 hpf. a. Spatial orientation of the fin buds and schematic of the deletion**. b.** Various samples are shown to illustrate the variability observed. Each WISH experiment was repeated independently twice with similar results. An attenuation that can be observed in distal most expression in homozygous mutant specimens contrasts with mice where expression in the autopod is always completely absent in the comparable deletion. Scale bar: 50 µm

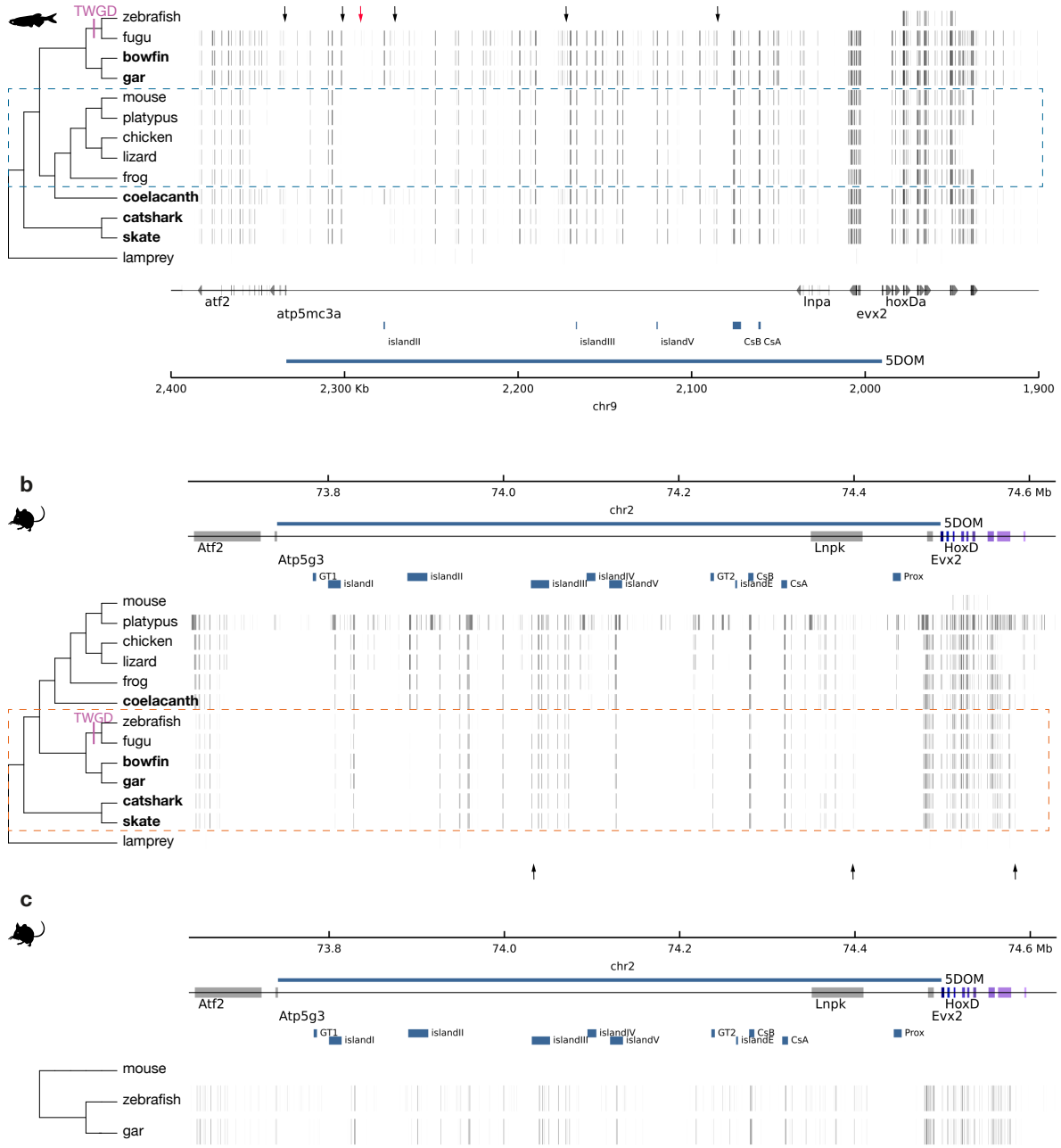

Supplementary Figure 2. Sequence conservation within 5DOM follows phylogenic distances. a. Whole genome alignments across 13 vertebrate species. The reference genome is zebrafish, conservation blocks in the reference genome indicate paralogous sequences (only seen in the *hoxda* cluster itself, on the top right). Phylogenic relationships are shown on the left by using a tree. Non-teleost fishes are in bold. TWGD: teleost-specific whole genome duplication. Tetrapod species are included into the large blue dashed rectangle. Conservation strictly follows phylogenic distances, with more closely related species having more conservation blocks. The black arrows indicate representative examples of sequences specifically lost in tetrapods. **b.** The same alignments as in panel **a** are projected onto the mouse genome. The large orange dashed rectangle includes cartilaginous and ray-finned fishes. The black arrows indicate the few examples of sequences that would have been lost specifically in zebrafish, or in teleosts at large. **c.** The mouse, zebrafish and gar 5DOM sequences are aligned and projected onto the mouse genome.

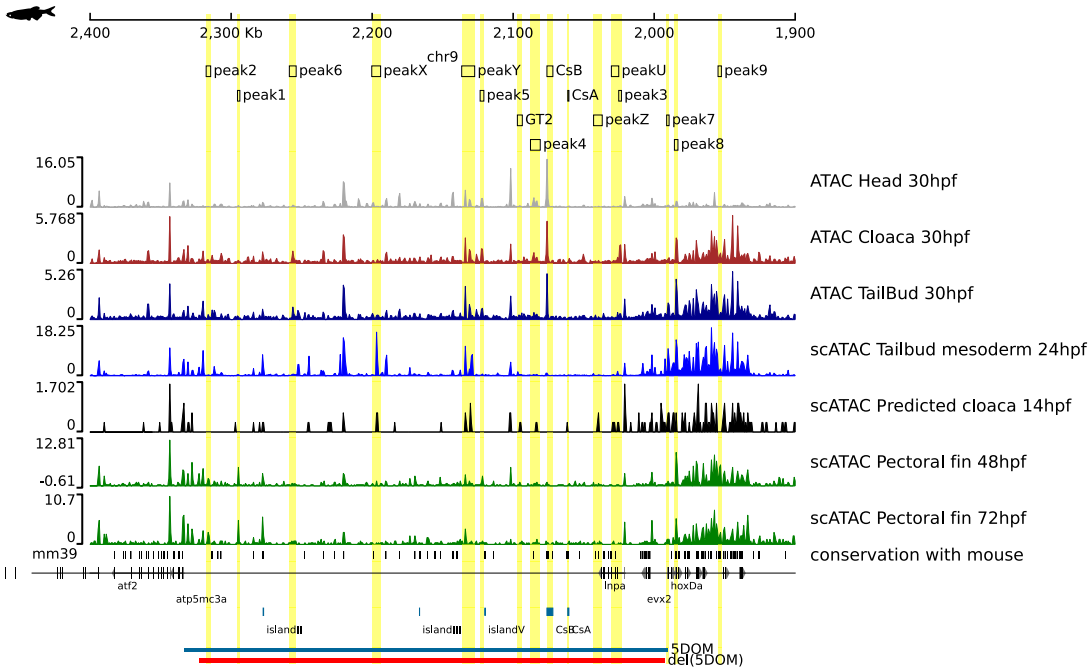

Supplementary Figure 3. Chromatin accessibility profiles of the zebrafish 5DOM. ATAC-seq and scATAC-seq data are shown over the zebrafish *hoxda* locus. Specific regions of accessibility within 5DOM are highlighted in yellow. The scATAC-seq data were obtained from ref[1] and the predicted cloaca cell annotations were assigned by transferring annotations from scRNA-seq endo.31 cluster data from ref[2] to scATAC-seq cells. While this increased cellular specificity led to the appearance of peaks not visible in our gross dissection, likely due to dilution effect, some peaks observed in our former material were clearly contaminants from tissues included in the samples and were no longer scored in the identified cell types (e.g., CsB, compare tracks 2 and 5).

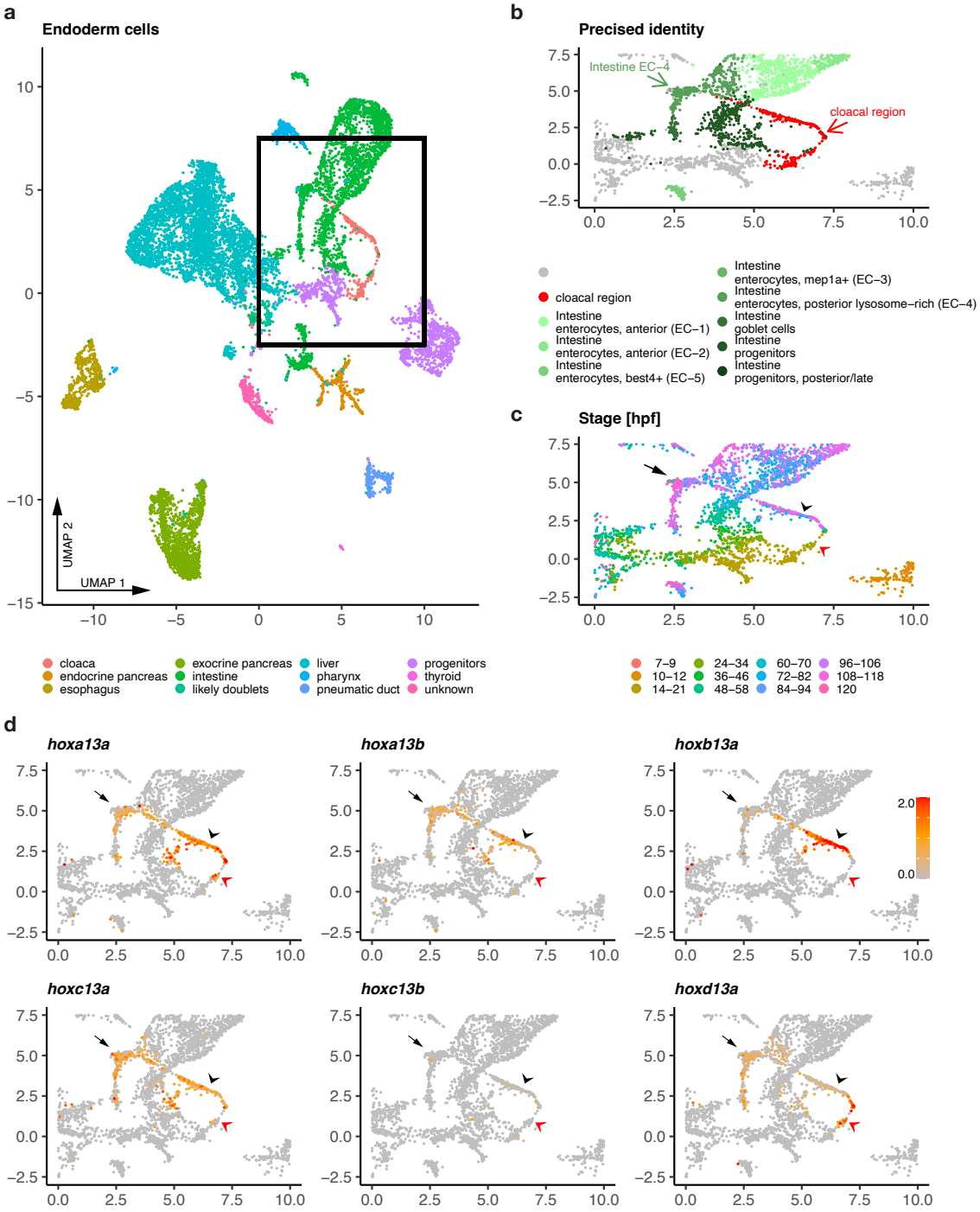

Supplementary Figure 4. *hox13* gene expression in the Daniocell atlas. a. UMAP of endoderm cells using matrices extracted from ref[2] colored by tissue. The black rectangle indicates the UMAP region which contains cellular clusters from the cloacal region. All other panels in the figure correspond to this rectangle. **b.** UMAP of endodermal cells and identities of their clusters. The colors indicate the identities of cells from both the cloacal region (red arrow) and the posterior intestine (dark green, arrow). **c.** UMAP of selected endoderm, clustered by developmental stages (color code below). **d.** UMAP as in panel **b**, with the expression in red of the various *hox13* paralogous genes. All cells with a normalized expression level above 2 are displayed in red. In panels **c** and **d**, arrowheads indicate *hox13* expressing cells in the cloacal region either at early (red) or late (black) timepoints. The black arrows point to *hox13* expression in intestinal cells.

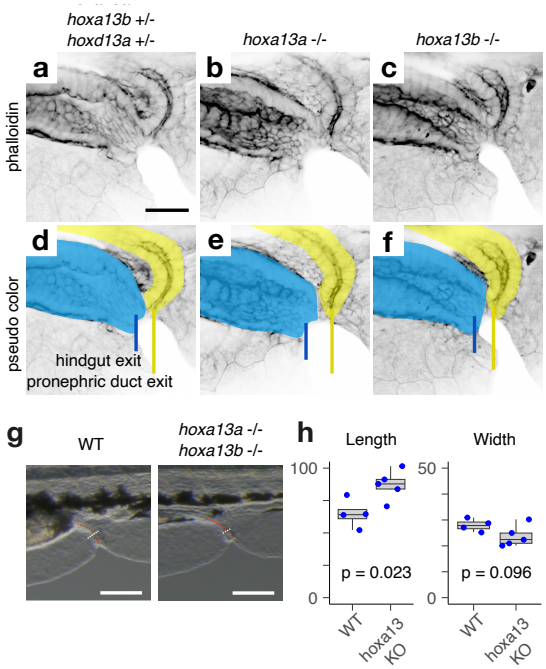

Supplementary Figure 5. Cloacal region phenotypes in *hox13* mutant zebrafish. a-f. Confocal micrographs of mutant cloacal regions at 6dpf shown in single channel (**a-c**) and pseudo color (**d-f**). **d.** Triple *hoxa13a*;*hoxa13b*;*hoxd13a* heterozygotes (n=6) as well as single homozygous *hoxa13a* mutants (**e**, n=7) exhibit a wild-type morphology with separate openings for the hindgut (blue) and pronephric duct (yellow). **f.** Homozygous *hoxa13b* single mutants also have wild-type morphology (n=7). **g-h.** Length and width of the hindgut and pronephric duct in wild-type and *hoxa13* mutant zebrafish embryos at 3 dpf. **g.** The length (red dotted lines) and width (white dotted lines) of the hindgut and pronephric complex at the median fin fold level were quantified in micrometers in wild-type (n=4, left) and *hoxa13a*;*hoxa13b* double mutant embryos (n=5, right). **h.** The length difference of the hindgut and pronephric complex between wild-type and *hoxa13* double mutant embryos is statistically significant (p=0.023, two-sided Welch's t-test). The boxes represent the interquartile range (IQR), with the lower and upper hinges denoting the first and third quartiles (25th and 75th percentiles). Whiskers extend from the hinges to the furthest data points within 1.5 times the IQR. The upper whisker reaches the largest value within this range, while the lower whisker extends to the smallest value within 1.5 times the IQR from the hinge. Scale bars: 30 µm in **a-f** and 100 µm in **g**.

References

1. Sun, K. *et al.* Mapping the chromatin accessibility landscape of zebrafish embryogenesis at single-cell resolution by SPATAC-seq. *Nat Cell Biol* **26**, 1187–1199 (2024).

2. Sur, A. *et al.* Single-cell analysis of shared signatures and transcriptional diversity during zebrafish development. *Developmental Cell* **58**, 3028-3047.e12 (2023).